Three-dimensional dimeron as a stable topological object

Yong-Kai Liu[1] and Shi-Jie Yang[1,2,*]

[1]*Department of Physics, Beijing Normal University, Beijing 100875, China*
[2]*State Key Laboratory of Theoretical Physics, Institute of Theoretical Physics, Chinese Academy of Sciences, Beijing 100190, China*

Searching for novel topological objects is always an intriguing task for scientists in various fields. We study a three-dimensional (3D) topological structure called a 3D dimeron in trapped two-component Bose-Einstein condensates. The 3D dimeron differs from the conventional 3D skyrmion for the condensates hosting two interlocked vortex rings. We demonstrate that the vortex rings are connected by a singular string and the complexity constitutes a vortex molecule. The stability of the 3D dimeron is examined in two different models using the imaginary time evolution method. We find that the stable 3D dimeron can be naturally generated from a vortex-free Gaussian wave packet incorporating a synthetic non-Abelian gauge potential into the condensates.

I. INTRODUCTION

Topological objects are often interesting topics in a variety of fields ranging from the condensed matter physics [1,2] and liquid crystals to particle physics and the modern universe [3,4]. Among them, Bose-Einstein condensation (BEC) of dilute atomic gases provides an ideal pilot to investigate the rich topological excitations [5]. Most of the important parameters such as dimensions, trapping potentials, and interactions between the atoms can be precisely tuned for the condensates in the experiments. There have been many experimental techniques that allow one to create kinds of exotic topological objects [5,6]. Another advantage of the alkali-metal atomic BECs is that they can be well described by the order parameters within the mean-field theory [7]. By using the normalized spinor $\xi(\mathbf{r})$ with $\xi^\dagger \xi = 1$, the order parameter (OP) is represented as $\psi(\mathbf{r}) = \sqrt{n(\mathbf{r})}\xi(\mathbf{r})$, where $n(\mathbf{r})$ is the density of the condensate. A rich variety of the OP manifolds admit various kinds of topological objects.

Three-dimensional (3D) skyrmions and knots which are topological solitons classified by the third homotopy group have been a fascinating subject for decades [7–9]. The 3D skyrmions, which are identified by counting the number covering the 3D sphere surface SU(2) $\simeq S^3$, have been studied widely [10–17]. Knots are identified by mapping from a three-dimensional sphere S^3 to S^2 and are classified by the homotopy classes with $\pi_3(S^2) \simeq Z$ [18–23]. Knots differ from other topological excitations such as vortices, monopoles, and skyrmions in that knots are classified by a linking number while others are classified by winding numbers.

Although the conventional 3D skyrmions in two-component BECs have been widely studied since their proposal, all of the wave functions have the same form along with the same asymptotic boundary condition [11,12]. In this paper, we investigate a configuration of 3D topological structure which we call the 3D dimeron, a terminology analogous with the 2D meron pair (sometimes named the 2D bimeron) in which two vortex cores are connected by a domain wall [24,25]. Mathematically, it is topologically not

possible to construct a single meron or half-skyrmion in the three-dimensional physical space. Under the requirement of compactness that all spin vectors should point to one direction at spatial infinity, we design in the wave function of each component a quantized ring-shape vortex that is interlocked [Fig. 1(a)]. The knotted topological object is characterized by a winding number with unit topological invariant. Furthermore, we find that the cores of interlocked vortex ring are connected by a singular string of the relative phase, similar to the string of the gauge potential in the Dirac's monopole. It constitutes a 3D vortex molecule.

The purpose of this paper is to systematically study the 3D dimeron in the trapped two-component BECs. The particles can convert into each other between the two components and the total particle number is conserved. The normalization of the wave function can be taken as $\int d\mathbf{r}(|\psi_1|^2 + |\psi_2|^2) = 1$. We numerically examine the stability of the 3D dimeron in two different models by evolving the coupled Gross-Pitaevskii equations (GPEs) using the imaginary time evolution method. For the first model with a coherent Rabi coupling between the two components, we find that the 3D dimeron can survive for more than 400 ms in the usual alkali-metal atomic condensates, which is long enough for the lifetime of BECs. In order to seek a truly stable topological object, in the second model we incorporate a 3D non-Abelian gauge potential into the condensates in which the 3D dimeron is naturally created.

The paper is organized as follows. In Sec. II we establish the notation of the 3D dimeron and analyze the topological structure and spin textures of the 3D dimeron in detail. In Sec. III we numerically study the stability of the 3D dimeron in a model where two-component Bose-Einstein condensates are coherently coupled. In Sec. IV we create a stable 3D dimeron from a vortex-free Gaussian wave packet via incorporating a synthetic non-Abelian gauge potential into the condensates. A brief summary is included in Sec. V.

II. 3D DIMERON TEXTURE

In the two-component BECs, the conventional 3D skyrmion is composed of a ring component and a line component with boundary values $\xi^\dagger = (1,0)$ for $\mathbf{r} \to \infty$ [12,13]. It is usually

---

*Corresponding author: yangshijie@tsinghua.org.cn
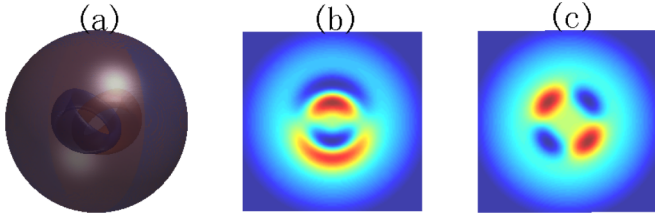
FIG. 1. (Color online) (a) Isosurface of density of ψ_1 (red [gray]) and ψ_2 (blue [dark gray]) from the ansatz wave function (1) with a Thomas-Fermi density profile. Each component hosts a ring-shaped interlocked vortex. The 2D density profiles of ψ_1 are (b) the x-y plane and (c) the x-z plane.

FIG. 2. (Color online) Spin texture of the 3D dimeron at different radii: (a) $r = 3$ and (b) $r = 10$. The color of the arrows indicate variation of the global $U(1)$ phase. At large enough distance from the center, all the arrows uniformly point in the x direction.

expressed as [11]

$$\begin{pmatrix} \psi_1(\mathbf{r}) \\ \psi_2(\mathbf{r}) \end{pmatrix} = \sqrt{n(\mathbf{r})}\,\hat{U}^\dagger(\mathbf{r})\begin{pmatrix} 1 \\ 0 \end{pmatrix}, \tag{1}$$

where $\hat{U}(\mathbf{r}) = \exp[i\lambda(\mathbf{r})\hat{\sigma}\cdot\hat{\mathbf{r}}]$ with $\hat{\sigma}$ being the Pauli matrices and $\hat{\mathbf{r}}$ being the unit vector. $\hat{U}(\mathbf{r})$ defines a map from the physical region R^3 to the OP space S^3. The map falls into the homotopy class, which is characterized by an integer-valued winding number,

$$W_{3D} = \frac{\varepsilon_{\alpha\beta\gamma}}{24\pi^2}\int d\mathbf{r}\,\mathrm{Tr}[\hat{U}(\partial_\alpha\hat{U}^\dagger)\hat{U}(\partial_\beta\hat{U}^\dagger)\hat{U}(\partial_\gamma\hat{U}^\dagger)]. \tag{2}$$

Before discussion of the 3D dimeron, we briefly review the 2D meron pair in a two-component BEC [24,25]. For atoms with two hyperfine states such as ^{87}Rb, the two condensates can be coherently coupled through a Rabi field. The 2D meron pair, which differs from the 2D skyrmion, is stabilized by the Rabi coupling [25]. The cores of the two vortices are connected by a domain wall of the relative phase to form a vortex molecule. Essentially, the coherent Rabi coupling term plays the role of a transverse magnetic field that aligns the spin along the x axis, leading to $\xi^\dagger \to (1,1)$ at distance far from the core region.

In order to construct the 3D dimeron, we consider the following form of OP:

$$\begin{pmatrix} \psi_1(\mathbf{r}) \\ \psi_2(\mathbf{r}) \end{pmatrix} = \sqrt{n(\mathbf{r})}\,\hat{V}^\dagger(\mathbf{r})\begin{pmatrix} 1/\sqrt{2} \\ 1/\sqrt{2} \end{pmatrix}, \tag{3}$$

where $\hat{V}(\mathbf{r}) = \exp[i\lambda(\mathbf{r})\hat{\sigma}\cdot\hat{v}(\theta,\phi)]$ with (r,θ,ϕ) being the spherical coordinates. It is illustrative to study the topological structure with the spherically symmetric ansatz by assuming $\lambda(0) = n\pi$ and $\lambda(\infty) = 0$. We take $\hat{v}(\theta,\phi) = (\cos\theta, \sin\theta\sin m\phi, -\sin\theta\cos m\phi)$ which determines a unique mapping: $S^2 \to S^2$. It should be noted that the unit vector $\hat{v}$ is *not* identical to the unit oriental vector $\hat{\mathbf{r}}$ in the 3D physical space. We demonstrate that the wave function (1) represents a spin configuration of the 3D dimeron topology. It is straightforward to prove that the winding number is $W_{3D} = mn$. In the present work, we focus on the simple case of $m = n = 1$.

Figure 1 show the density distributions of the ansatz wave function (1) with a global Thomas-Fermi density profile. In contrast to the picture of a ring component and a line component in the conventional 3D skyrmion, each component hosts a ring-shaped vortex that interlocks [the inner part of Fig. 1(a)]. Figures 1(b) and 1(c) are the 2D density
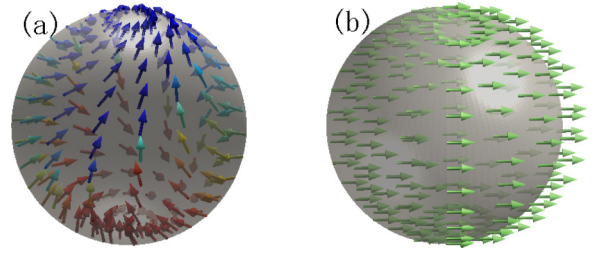
distributions of component ψ_1 in the x-y plane and the x-z plane, respectively. The density peaks of one component locates at the vortex core of the other component. This results in a structure in which the total density has no zeros in the space.

The pseudospin representation of the order parameter with internal degrees of freedom is useful to obtain a physical interpretation by mapping the system to a magnetic system. In our case, an insight into the 3D dimeron can be gained as the two-component BECs with the total normalization are described as spin-1/2 BEC [24,25]. Figure 2 displays the spin texture of the 3D dimeron, where the pseudospin is defined by $\mathbf{S}(\mathbf{r}) = \xi^\dagger(\mathbf{r})\hat{\sigma}\xi(\mathbf{r})$ [1,26,27]. The color of the arrows indicate the variation of the global $U(1)$ phase. The $U(1)$ phase is taken as the fourth component of the unit 4-vector since the 3-vector $\mathbf{S}$ is not enough to describe the S^3 manifold. The pseudospin vector $\mathbf{S}(\mathbf{r})$ are twisted in the central region and gradually point to the $(1,0,0)$ direction at larger distance from the center. The global phase $\Phi(\mathbf{r})$ becomes uniform, which leads to a vanishing relative phase between the two condensates. As shown in Fig. 2(b) $S_x \to 1$ while $\Phi \to 0$ as $r \to \infty$, which fulfills the compactness of the OP manifold, $\xi^\dagger = (1,1)$.

To get a better view of the 3D spin texture, we illustrate the 2D spin texture in the $z = 0$ plane [Fig. 3(a)] and the $y = 0$ plane [Fig. 3(b)]. Here the color of the arrows specify the values of S_z. In the $y = 0$ plane, all arrows point to $(1,0,0)$ at large radius whereas there is a pair of vortex cores in either the left or the right half-plane which are highlighted by $S_z = 1$ (red [gray]) and $S_z = -1$ (blue [dark gray]). As addressed in Refs. [24,25], the pair of vortex cores are connected by a domain wall. Consequently, this cross section reveals a 2D
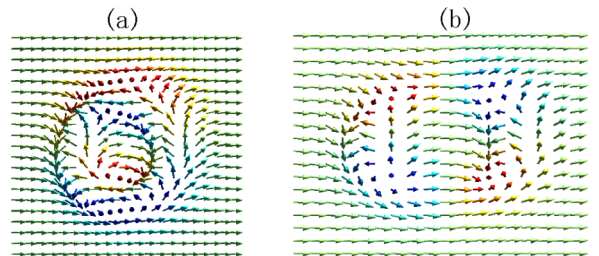
FIG. 3. (Color online) Texture of $\mathbf{S}(\mathbf{r})$ in (a) the $z = 0$ plane and (b) the $y = 0$ plane. The color of the arrows specifies the magnitude of S_z.
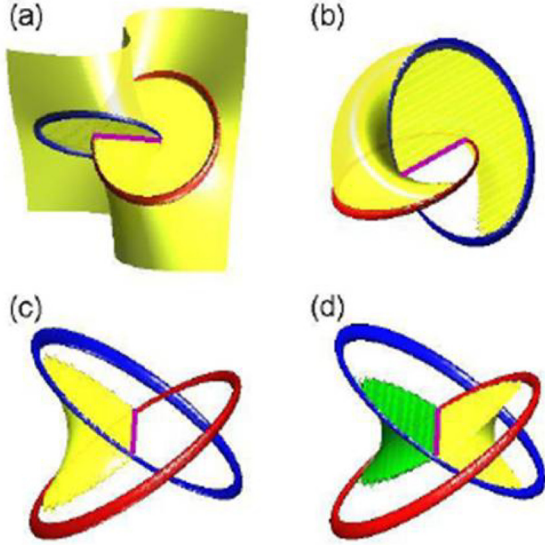
FIG. 4. (Color online) Isosurface of the relative phase between the two components: (a) $\vartheta = 0$, (b) $\vartheta = \pi/2$, (c) $\vartheta = 4\pi/3$, and (d) $\vartheta = -3\pi/2$ and $\vartheta = 3\pi/2$ (green [gray]), respectively. The red and blue loops (gray and dark gray) are the cores of the vortex ring in each component. The purple (dark gray) line is a common segment of all isosurfaces, which implies it is not well defined and constitutes a singular string.

meron pair with a topological charge $W_{2D} = \frac{1}{4\pi} \int \mathbf{S} \cdot (\partial_\rho \mathbf{S} \times \partial_z \mathbf{S}) d\rho dz = 1$. Generally, there is a 2D meron pair in all of the vertical half-planes. Based on this analogy, we name the 3D texture in Fig. 2 with the terminology of 3D dimeron. We mention that in the conventional 3D skyrmion there is a 2D skyrmion in each vertical half-plane [13].

We examine the distribution of the relative phase between the two components $\vartheta(\mathbf{r}) = \theta_1(\mathbf{r}) - \theta_2(\mathbf{r})$. Figures 4(a)–4(c) display the isosurfaces of the relative phase for (a) $\vartheta = 0$, (b) $\vartheta = \pi/2$, (c) $\vartheta = 4\pi/3$, and (d) $\vartheta = -3\pi/2$ and $\vartheta = 3\pi/2$ (green [gray]), respectively. It is remarkable that there is a common segment (the purple [dark gray] line) of all the isosurfaces of the relative phase. This segment connects the cores of the two vortex rings. It is ill defined since on the segment the value of the relative phase is indefinite. The singular string is just like that in the Dirac's monopole where a singular string presents in the gauge potential. This feature essentially distinguishes the 3D dimeron from the conventional 3D skyrmion. It demonstrates that the twisted complexity is not simply two interlocked vortex rings but constitutes a 3D vortex molecule.

It is also interesting to point out that the 3D dimeron shows a knotted spin texture which is topological nontrivial texture with a Hopf charge $\pi_3(S^2) \simeq Z$, where S^2 is a two-dimensional sphere whose point specifies the direction of the pseudospin $\mathbf{S}$ [2]. As shown in Fig. 5, the torus is the preimage of $S_x = 0$ in the real space. We attach on the surface with color to indicate the value of $\varphi(\mathbf{r}) = \arctan(S_y/S_z)$ (the vector orientation on this surface), which exactly exhibits the chirality of the knot. The two loops on the torus are the preimages of $\mathbf{S} = (0,1,0)$ (yellow [light gray]) and $\mathbf{S} = (0,0,1)$ (red [gray]), respectively, while the loop in the inner of the torus
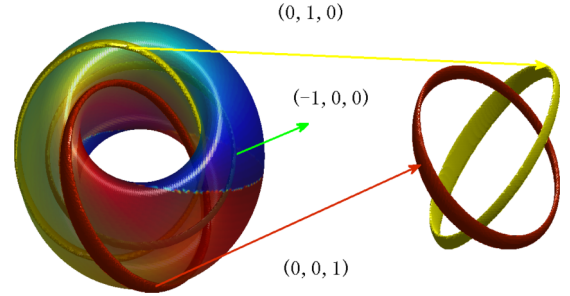
FIG. 5. (Color online) The knotted topology of the 3D dimeron: The torus is the preimage isosurface of $S_x = 0$. The variations of color on the torus specify the angle between S_z and S_y which reflect chirality of the knot. The yellow (light gray), red (gray), and green (dark gray) loops are the preimages of $\mathbf{S} = (0,1,0)$ and $\mathbf{S} = (0,0,1)$, and $\mathbf{S} = (-1,0,0)$, respectively. They are pairwise interlocked.

is the preimage of $\mathbf{S} = (-1,0,0)$ (green [dark gray]). Any two loops interlock once and only once, as illustrated in the right part of the figure. It implies a topological mapping that falls into the nontrivial homotopy class $\pi_3(S^2) \cong Z$ and is characterized by a topological invariant called the Hopf charge: $Q_H = \frac{1}{4\pi^2} \int \varepsilon_{ijk} \mathcal{F}_{ij} \mathcal{A}_k$, where $\mathcal{F}_{ij} = \partial_i \mathcal{A}_j - \partial_j \mathcal{A}_i = \mathbf{S} \cdot (\partial_i \mathbf{S} \times \partial_j \mathbf{S})$. Two loops corresponding to the preimages of any two distinct points on the target S^2 linked one times indicate that $Q_H = 1$. This can be directly verified by computing the quantity with the ansatz wave function (1).

In the literature on skyrmions and knots, stability and existence of a solution are usually taken to mean the energetic stability [28]. Just like the conventional 3D skyrmion, the 3D dimeron may be energetically unstable against shrinking to zero size [11]. In the next sections, we examine the energetic stability of the 3D dimeron in two different models.

III. STABILITY ANALYSIS

As the 2D meron pair can be stabilized by the Rabi coupling, we guess it still works for the 3D dimeron. Suppose the condensates are trapped in a 3D well and are coherently coupled by a Rabi field. The Rabi field plays the role of an external magnetic field along the x direction, which stabilizes the boundary constraint on the system. The dynamics is governed by the coupled GPEs,

$$i\hbar \frac{\partial \psi_i}{\partial t} = \left(-\frac{\hbar^2}{2m} \nabla^2 + V(\mathbf{r}) + \sum_{j=1,2} U_{ij} |\psi_j|^2 \right) \psi_i - \hbar \omega_R \psi_j, \tag{4}$$

where ψ_i $(i = 1,2)$ denotes the wave functions of the two components and ω_R is the Rabi frequency. The external potential takes an axisymmetric harmonic oscillator $V(\mathbf{r}) = \frac{1}{2} m\omega^2(x^2 + y^2) + \frac{1}{2} m\omega_z^2 z^2$. The constants $U_{ij} = 4\pi \hbar^2 a_{ij}/m$ represent the intraspecies $(i = j)$ and interspecies $(i \neq j)$ interactions. It is convenient to simplify the equations in the unit scale as [15]

$$i \frac{\partial \psi_i}{\partial t} = -\frac{1}{2} \nabla^2 \psi_i + \tilde{V}(\mathbf{r}) + \sum_{j=1,2} \gamma_{ij} |\psi_j|^2 \psi_i - \omega_R \psi_j. \tag{5}$$

To examine the energetic stability of the 3D dimeron, we numerically evolve the coupled GPEs (5) in the imaginary time with the constraint of the constant total number. The evolution leads to a final state which minimizes the energy functional. We adopt the split-step method according to the decomposition $e^{-\triangle t \hat{H}} = e^{-\frac{\triangle t}{2}\hat{T}} e^{-\triangle t \hat{V}_{\text{int}}} e^{-\frac{\triangle t}{2}\hat{T}}$ [29–31]. Here $\hat{T}$ is the kinetic part and $\hat{V}_{\text{int}}$ is the remaining part of the Hamiltonian. For the present case, $e^{-\triangle t \hat{V}_{\text{int}}}$ can be further factorized into $e^{-\frac{\triangle t}{2}\hat{V}'} e^{-\triangle t \hat{V}_{\text{Rabi}}} e^{-\frac{\triangle t}{2}\hat{V}'}$, where $\hat{V}' = \hat{V}_{\text{int}} - \hat{V}_{\text{Rabi}}$. We use $\gamma_{11} = \gamma_{22} = \gamma_{12} = 10\,000$, $\omega_R = 0.7$, and the initial 3D dimeron state (1) with a Thomas-Fermi density profile for a spatial grids of $151 \times 151 \times 151$. We trace the topological invariant during the imaginary-time evolution to check the stability of the 3D dimeron. The two vortex rings move and their radii shrink until they touch at $\tau = it \simeq 420$ ms for a realistic trap $\omega = \omega_z = 2\pi \times 7$ Hz when the two vortex rings are unlocked and the 3D dimeron is destroyed. The shrinking instability was previously reported in Ref. [32]. We also find that the Rabi coupling can help to slacken the decay of the 3D dimeron. Although unstable, it does not imply that the 3D dimeron cannot be experimentally observed since the typical scale of survival time is long enough for the realistic condensates. As a comparison, a 2D skyrmion in an antiferromagnetic spinor BEC was observed in experiments, although it is energetically unstable [33].

IV. STABLE DIMERON CREATED IN A NON-ABELIAN GAUGE FIELD

In order to seek a really stable 3D dimeron, we attempt an alternative way. We take account of a synthetic non-Abelian gauge potential, which recently has been a popular topic in ultracold atoms. The essence of the 3D dimeron is the interlocked vortex rings in each component. Inspired by the form of the SU(2) transformation $\hat{V}(\mathbf{r})$ in Eq. (1), we configure the following non-Abelian gauge potential,

$$\mathbf{A} = \kappa_1 \sigma_x \mathbf{e}_z + \kappa_2 \sigma_y \mathbf{e}_y - \kappa_3 \sigma_z \mathbf{e}_x. \tag{6}$$

The energy functional of the condensates incorporating the above non-Abelian gauge potential reads

$$E = \frac{1}{2} \int [\mathbf{D}\psi(\mathbf{r})]^{\dagger} \cdot [\mathbf{D}\psi(\mathbf{r})] d\mathbf{r}$$
$$+ \int \left[\frac{1}{2} r^2 n(\mathbf{r}) + \gamma n^2(\mathbf{r}) \right] d\mathbf{r}, \tag{7}$$

where the covariant derivative is defined by $\mathbf{D} = (-i \bigtriangledown + \mathbf{A})$. The energy functional (7) has the symmetry for the combined rotation of the real space and the spin space. In analogy to the argument of the helical OP modulation [17,34], a 3D dimeron state may be created in the present model with appropriate coupling strength.

Our numerical simulations confirm that a 3D dimeron is indeed created. Figure 6 displays the resultant density profile of the two-component BECs after the imaginary-time evolution
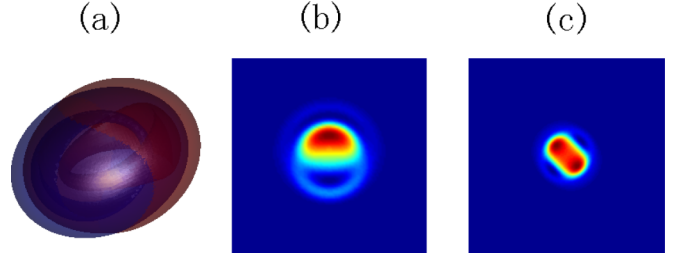
FIG. 6. (Color online) The spatial profile of a stable 3D dimeron generated by the imaginary-time evolution of the GPEs with the non-Abeian gauge potential (6). (a) Isosurface of the density for ψ_1 (red [gray]) and ψ_2 (blue [dark gray]), where two interlocked vortex rings are evident. The 2D density profiles of ψ_1 in (b) the x-y plane and (c) the x-z plane are similar to those in Fig. 1.

of the GPEs generated from the energy functional (7). It evidently reveals the typical topological structure of two interlocked vortex rings just as in Fig. 1 and demonstrates the creation of a stable 3D dimeron. In the simulations, the initial state is taken as a vortex-free Gaussian wave packet with a uniform spinor $\xi^{\dagger} = (1,1)$. We have chosen the parameters $\gamma = 100$ and $\kappa_1 = \kappa_2 = \kappa_3 = 2.2$ and fixed the total particle number of the two components.

Ruostekoski proposed a method of generating a 3D skyrmion in a trapped BEC using electromagnetic fields, mainly including creation of a singly quantized vortex and a vortex ring [11]. Several experimental schemes of creating vortex rings in the atomic BECs, such as interference of two-component BECs and rotating quadrupole magnetic fields, have been successfully tested [35–40]. In order to create a 3D dimeron, we need to generate two vortex rings in the two-component BECs. An alternative way to create the 3D dimeron is to design a synthetic non-Abelian gauge potential of the form (6) by dressed states via proper Ramam transitions in the ultracold atoms. The relevant setups are under investigation.

V. SUMMARY

In summary, we have presented a configuration of 3D topological structure named a 3D dimeron. It contains a string and constitutes a vortex molecule. We demonstrated a way of creating a stable 3D dimeron by incorporating a non-Abelian gauge potential into the two-component condensates. The method can be extended to construct similar topological objects in the spinor BECs with large spin degree of freedom which can produce more interlocked vortex rings. Finally, we note that similar configurations were investigated in superconductivity [32,41].

[1] E. Babaev, L. D. Faddeev, and A. J. Niemi, Phys. Rev. B **65**, 100512 (2002).

[2] Y. Kawaguchi, M. Nitta, and M. Ueda, Phys. Rev. Lett. **100**, 180403 (2008).

[3] J. Jäykkä and J. Hietarinta, Phys. Rev. D **79**, 125027 (2009).

[4] A. Vilenkin and E. P. S. Shellard, *Cosmic Strings and Other Topological Defects* (Cambridge University Press, Cambridge, UK, 1994).

[5] Y. Kawaguchi, M. Kobayashi, M. Nitta, and M. Ueda, Prog. Theor. Phys. Suppl. **186**, 455 (2010).

[6] K. Kasamatsu, H. Takeuchi, M. Tsubota, and M. Nitta, Phys. Rev. A **88**, 013620 (2013).

[7] Y. Kawaguchi and M. Ueda, Phys. Rep. **520**, 253 (2012).

[8] T. H. R. Skyrme, Proc. R. Soc. London A **260**, 127 (1961).

[9] T. H. R. Skyrme, Nucl. Phys. **31**, 556 (1962).

[10] U. A. Khawaja and H. T. C. Stoof, Nature (London) **411**, 918 (2001).

[11] C. M. Savage and J. Ruostekoski, Phys. Rev. Lett. **91**, 010403 (2003).

[12] J. Ruostekoski and J. R. Anglin, Phys. Rev. Lett. **86**, 3934 (2001).

[13] Y.-K. Liu, S. Feng, and S.-J. Yang, Euro. Phys. Lett. **106**, 50005 (2014).

[14] R. A. Battye, N. R. Cooper, and P. M. Sutcliffe, Phys. Rev. Lett. **88**, 080401 (2002).

[15] S. Wüester, T. E. Argue, and C. M. Savage, Phys. Rev. A **72**, 043616 (2005).

[16] I. F. Herbut and M. Oshikawa, Phys. Rev. Lett. **97**, 080403 (2006).

[17] T. Kawakami, T. Mizushima, M. Nitta, and K. Machida, Phys. Rev. Lett. **109**, 015301 (2012).

[18] L. Faddeev and A. J. Niemi, Nature (London) **387**, 58 (1997).

[19] J. Gladikowski and M. Hellmund, Phys. Rev. D **56**, 5194 (1997).

[20] R. A. Battye and P. M. Sutcliffe, Phys. Rev. Lett. **81**, 4798 (1998).

[21] J. Hietarinta and P. Salo, Phys. Lett. B **451**, 60 (1999).

[22] Y. M. Cho, H. Khim, and P. Zhang, Phys. Rev. A **72**, 063603 (2005).

[23] Y.-K. Liu and S.-J. Yang, Phys. Rev. A **87**, 063632 (2013).

[24] K. Kasamatsu, M. Tsubota, and M. Ueda, Phys. Rev. Lett. **93**, 250406 (2004).

[25] K. Kasamatsu, M. Tsubota, and M. Ueda, Phys. Rev. A **71**, 043611 (2005).

[26] M. Hindmarsh, Nucl. Phys. B **392**, 461 (1993).

[27] A. J. Niemi, K. Palo, and S. Virtanen, Phys. Rev. D **61**, 085020 (2000).

[28] G. H. Derrick, J. Math. Phys. **5**, 1252 (1964).

[29] W. Bao, D. Jaksch, and P. A. Markowich, J. Comput. Phys. **187**, 318 (2003).

[30] W. Bao and H. Wang, J. Comput. Phys. **217**, 612 (2006).

[31] S.-J. Yang, Q.-S. Wu, S.-N. Zhang, and S. Feng, Phys. Rev. A **77**, 033621 (2008).

[32] J. Jäykkä, J. Hietarinta, and P. Salo, Phys. Rev. B **77**, 094509 (2008).

[33] J.-Y. Choi, W. J. Kwon, and Y.-I. Shin, Phys. Rev. Lett. **108**, 035301 (2012).

[34] T. Kawakami, T. Mizushima, and K. Machida, Phys. Rev. A **84**, 011607(R) (2011).

[35] B. Jackson, J. F. McCann, and C. S. Adams, Phys. Rev. A **61**, 013604 (1999).

[36] F. Pinsker, N. G. Berloff, and V. M. Pérez-García, Phys. Rev. A **87**, 053624 (2013).

[37] A. I. Yakimenko, Yu. M. Bidasyuk, O. O. Prikhodko, S. I. Vilchinskii, E. A. Ostrovskaya, and Yu. S. Kivshar, Phys. Rev. A **88**, 043637 (2013).

[38] B. P. Anderson, P. C. Haljan, C. A. Regal, D. L. Feder, L. A. Collins, C. W. Clark, and E. A. Cornell, Phys. Rev. Lett. **86**, 2926 (2001).

[39] N. S. Ginsberg, J. Brand, and L. V. Hau, Phys. Rev. Lett. **94**, 040403 (2005).

[40] I. Shomroni, E. Lahoud, S. Levy, and J. Steinhauer, Nat. Phys. **5**, 193 (2009).

[41] J. Jäykkä and J. M. Speight, Phys. Rev. D **84**, 125035 (2011).